Published in final edited form as:
Curr Drug Metab. 2012 January ; 13(1): 120–128.

Design of Curcumin loaded Cellulose Nanoparticles for Prostate Cancer

Murali Mohan Yallapu[1], **Mitch Ray Dobberpuhl**[1], **Diane Michele Maher**[1], **Meena Jaggi**[1,2], and **Subhash Chand Chauhan**[1,2,*]

[1]Cancer Biology Research Center, Sanford Research/University of South Dakota, Sioux Falls, SD 57104, USA

[2]Department of OB/GYN and Basic Biomedical Science Division, Sanford School of Medicine, University of South Dakota, Sioux Falls, SD 57104, USA

Abstract

Prostate cancer (PC) is the most frequently diagnosed disease in men in the United States. Curcumin (CUR), a natural polyphenol, has shown potent anti-cancer efficacy in various types of cancers. However, suboptimal pharmacokinetics and poor bioavailability limit its effective use in cancer therapeutics. Several successful CUR nanoformulations have recently been reported which improve upon these features; however there is no personalized safe nanoformulation for prostate cancer. This study contributes two important scientific aspects of prostate cancer therapeutics. The first objective was to investigate the comparative cellular uptake and cytotoxicity evaluation of β-cyclodextrin (CD), hydroxyl propyl methyl cellulose (cellulose), poly(lactic-*co*-glycolic acid) (PLGA), magnetic nanoparticles (MNP), and dendrimer based CUR nanoformulations in prostate cancer cells. Curcumin loaded cellulose nanoparticles (cellulose-CUR) formulation exhibited the highest cellular uptake and caused maximum ultrastructural changes related to apoptosis (presence of vacuoles) in prostate cancer cells. Secondly, the anti-cancer potential of the optimized cellulose-CUR formulation was evaluated in cell culture models using cell proliferation, colony formation and apoptosis (7-AAD staining) assays. In these assays, the cellulose-CUR formulation showed improved anti-cancer efficacy compared to free curcumin. Our study shows, for the first time, the feasibility of cellulose-CUR formulation and its potential use in prostate cancer therapy.

Keywords

Drug delivery systems; nanoparticles; cellulose; cancer therapy; nanomedicine; anti-cancer drug

1. INTRODUCTION

Prostate cancer (PC) is highly prevalent among cancer related diseases in the United States (153 per 100,000 persons) and the third leading cause of the cancer related death in men [1–3]. Efficient treatment for PC includes surgery, chemotherapy, radiation, prostate specific membrane antigen (PSMA) targeted therapy, and combination therapies [4–10]. Chemotherapy is considered a major therapeutic modality in which various natural and synthetic cyto-toxic drugs are used. However, conventional chemotherapeutic approaches are greatly limited due to their low therapeutic index, severe side effects, poor

*Address correspondence to this author at the Cancer Biology Research Center, Sanford Research/University of South Dakota, 2301 E. 60th Street North, Sioux Falls, SD 57104-0589, USA; Tel: 1-605-312-6106; Fax: 1-605-312-6071; Subhash.Chauhan@sanfordhealth.org; subhash.chauhan@usd.edu.

pharmacokinetics and consequent bio-pharmaceutical underperformance in the body [11–14]. In addition, most of these chemotherapeutics are suitable to treat localized androgen-dependent prostate cancers but exhibited limited efficacy in androgen-independent and metastatic prostate cancers [15–17]. Therefore, novel treatment modalities need to be developed that can treat all types of prostate cancers. Nanomedicine or nanoparticle drug delivery systems (NDDS) may improve these aspects of chemotherapy for prostate cancer patients [18–20].

Recent literature and clinical trials reveal that curcumin (CUR) (a yellow polyphenol extracted from the rhizome of turmeric, *Curcuma longa*) can be efficiently used to treat a variety of cancers such as prostate, breast, pancreatic, colorectal, gastric and cervical carcinomas [21–23]. The inhibition of carcinogenesis by CUR is achieved *via* influencing multiple mechanisms such as nuclear factor-kappaB (NF-kB), transcription factor activator protein-1 (AP-1), mitogen activated protein kinase (MAPK), tumor protein 53 (p53), nuclear β-catenin signaling, and AKT signaling pathways [24, 25]. CUR has proven to suppress the expression of epidermal growth receptor and estrogen receptors which are cancer associated growth factors [26]. Some proof-of-concept studies demonstrate that CUR efficiently sensitizes tumor cells to first line chemotherapies and radiation [27–29]. Furthermore, CUR is also shown to overcome multidrug resistance phenomenon in cancer therapeutics through down regulation of P-glycoprotein (P-gp) expression [30]. In addition, CUR has shown dose dependant (2.5–80 μM) effects on cancer cells while avoiding toxicity to normal cells [31]. Despite these encouraging properties, the use of CUR in clinical cancer treatment has not been fully actualized owing to its limitations related to low half-life, low serum levels, poor uptake and biodistribution in body [25].

To address these aspects of CUR, nanomedicine may be used to develop efficient therapeutic strategies for cancer treatments. In this direction, CUR nanoformulations of micelles, globular proteins, polymer nanoparticles, nanogel, and magnetic nanoparticles have demonstrated comparable/greater *in vitro* and *in vivo* biological activities compared to that of free CUR [32–37]. These sustained-release CUR nanoformulations offer improved availability and reduce the required dose of CUR for cancer therapy. Although a number of CUR nanoformulations have been reported in the literature, so far there has been no comparative study to evaluate which formulation(s) is more suitable for personalized prostate cancer therapy. Our central goal is to develop a nanoformulation with increased efficacy in prostate cancer treatment. Therefore, we examined the synthesis, characterization and comparative evaluation of β-cyclodextrin (CD), hydroxyl propyl methyl cellulose (cellulose), poly(lactic-*co*-glycolic acid) (PLGA), magnetic nanoparticles (MNP), and dendrimer CUR nanoformulations with free CUR using cellular uptake and cyto-toxicity studies in prostate cancer cells. The cellulose-CUR nanoformulation demonstrated maximum anti-cancer activity and induced marked ultrastructural changes related to cellular apoptosis in prostate cancer cells. These results indicate that a cellulose-CUR nanoformulation could be an effective nanoparticle delivery system in prostate cancer cells.

2. EXPERIMENTAL

2.1. Materials

β-cyclodextrin, hydroxyl propyl methyl cellulose (cellulose, M.W. 10,000, methoxy, 1.8–2.0 and propylene oxide 0.2–0.3, viscosity 2wt% in water 5 cps), poly(vinyl alcohol) (PVA) (M.W. 30,000–70,000), poly(L-lysine) (PLL) (M.W. 30,000–70,000), Fe(III) chloride hexahydrate (99%), Fe(II) chloride tetrahydrate (99%), ammonium hydroxide (28% w/v in water), pluronic polymer (F127), CUR (≥95% purity, (E, E)-1,7-bis(4-hydroxy-3-methoxyphenyl)-1,6-heptadiene-3,5-dione), acetone (≥99.5, ACS reagent grade), dimethylsulfoxide (DMSO) (ACS reagent, UV spectrophotometry grade, ≥99.9%) were

purchased from Sigma Chemical Co. (St. Louis, MO, USA). PLGA (50:50 lactide–glycolide ratio; inherent viscosity 1.32 dL/g at 30 °C) was purchased from Birmingham Polymers (Pelham, AL, USA). All chemicals were used as received without further purification.

2.2. Cell Lines

The human prostate cancer cell lines [(C4-2 and LNCaP (metastatic); DU-145 and PC-3 (non-metastatis)] were kindly supplied by Dr. Meena Jaggi (Sanford Research/USD, Sioux Falls). These cancer cells were maintained as monolayer cultures (C4-2, LNCaP and PC-3) in RPMI-1640 medium or in minimum essential medium (MEM, DU145, HyClone Laboratories, Inc., Logan, UT, USA) supplemented with 10% fetal bovine serum (Atlanta Biologicals, Lawrenceville, GA, USA) and 1% penicillin/streptomycin (Gibco BRL, Grand Island) at 37 °C in a humidified atmosphere (5% CO2).

2.3. Curcumin Nanoformulations

β-Cyclodextrin-curcumin (CD-CUR/CD30), poly(lactic-*co*-glycolic acid) curcumin (PLGA-CUR/NCUR6), magnetic nanoparticle-curcumin (MNP-CUR/F127250) nanoformulations were prepared according to our reported procedures [33, 38, 39]. Cellulose curcumin (cellulose-CUR) nanoformulation was prepared at a ratio of cellulose:curcumin (8:2, wt./wt.). First, cellulose (40 mg) was dissolved in 8 mL of deionized water in a glass vial (Fisher Scientific, Pittsburgh, PA, USA) with a magnetic bar. Curcumin (8 mg) dissolved in 500 mL acetone was added dropwise to aqueous cellulose solution while stirring at 400 rpm. The solution was stirred overnight, passed through a 0.45 mm Millex poly(vinylidene fluoride) (PVDF) syringe-driven filter unit (Millipore Corporation, Bedford, MA, USA), and the supernatant containing cellulose-CUR nanoformulation was recovered by freeze-drying (Labconco Freeze Dry System; − 48 °C, 133×10^{-3} mbar; Labconco, Kansas City, MO, USA). This procedure was adopted to prepare dendrimer-curcumin nanoformulation. All these curcumin nanoformulations were stored at 4 °C.

2.4. Compatibility of CUR Nanoformulations

The compatibility of curcumin in nanoformulations was evaluated by optical microscopy. In this study, two drops of 500 μg/mL of CUR or CUR in nanoformulations were placed onto a glass slide and dried at room temperature. These samples on glass slides were examined using optical microscopy (Olympus BX 41 microscope; Olympus, Center Valley, PA, USA). All the images were taken at 200× magnification.

2.5. Characterization of CUR Nanoformulations

The shape and morphology of CUR nanoformulations were investigated by JEOL-1210 transmission electron microscopy (TEM) (JEOL, Tokyo, Japan) operating at 80 kV. For this study, the suspension of nanocurcumin formulations (2–3 drops) were placed on the surface of 200 mesh formvar-coated copper TEM grid (grid size: 97 μm) (Ted Pella, Inc., Redding, CA, USA) and dried at room temperature prior to imaging of the nanoparticles.

Fourier transform infrared (FTIR) spectroscopy was employed to analyze the surface chemistry as well as to understand the chemical structure of CUR nanoformulations. The absorption spectrum was obtained using a Smiths Detection IlluminatIR FTIR microscope (Danbury, CT, USA) with diamond ATR objective. The CUR nanoformulations (powder) were scanned from 750 to 4000 cm^{-1} with a resolution of 4 cm^{-1}. The average of 32 scans for each sample was reported as FTIR spectra.

To understand the physical nature of CUR nanoformulations (powder), X-ray diffraction (XRD) and differential scanning calorimetry (DSC) methods were employed. XRD analysis of CUR nanoformulations were recorded using a D/Max-B Rikagu diffractometer (Rigaku

Americas Corp, Woodlands, TX) using Cuα radiation at λ = 0.1546 nm, running at 40 kV and 40 mA. Differential scanning calorimetry (DSC) analysis was performed on a Perkin Elmer simultaneous thermal analyzer STA6000. DSC patterns of the samples were recorded from 25 °C to 300 °C at a heating rate of 10 °C, under a constant nitrogen gas flow (100 mL/min).

2.6. Assessment of Cellular Uptake of CUR Nanoformulations

PC-3 cells (5×10^5) were cultured in the 6-well plates in 2 mL medium and allowed to attach overnight. The adherent cells were washed twice with PBS and then treated with CUR nanoformulations (10 or 20 μM) in 2 ml RPMI-1640 medium. After 6 hrs incubation, the cells were washed twice with PBS, trypsinized, centrifuged and collected in 2 ml media. In order to estimate the efficacy of nanoCUR formulations uptake, the cell suspensions (50 μL) were injected into an Acuri C6 Flow Cytometer (Accuri Cytometer, Inc., Ann Arbor, MI, USA) to determine the fluorescence levels due to curcumin in FL1 channel (488 excitation, Blue laser, 530 ± 15 nm, FITC/GFP). Standard deviations were calculated from 3 replicates.

2.7. Toxicity Evaluation of CUR Nanoformulations by TEM

For a comparative cyto-toxicity evaluation of CUR nanoformulations, PC-3 cells (1×10^7 cells per 150 mm plate) were cultivated in 150 mm plates in 20 mL medium and allowed to attach overnight. The adherent cells were washed twice with PBS. Then 20 mL of 20 μM CUR nanoformulations or equivalent amounts of nanoparticles without CUR in RPMI-1640 medium were replaced. The treated cells were trypsinized, centrifuged and fixed with standard formaldehyde (4%)-glutaraldehyde (1%) solution followed by OsO_4 solution. These cells were then dehydrated in a graded series of acetone and embedded in Spurr resin. These cell-containing resin blocks were sectioned using an ultramicrotome and ultrathin sections (70–90 nm thickness) were transferred onto TEM grid (grid size: 97μm) (Ted Pella Inc., Redding, CA, USA). The grids were processed with uranyl acetate and lead acetate solutions to visualize cellular ultra structures to evaluate the effects of CUR nanoformulations on cancer cells.

2.8. In vitro Anti-Cancer Effects

The cyto-toxicity of cellulose-CUR formulation was determined using a standard 3-(4,5-dimethylthiazol-2yl)-2,5-diphenyltetrazolium bromide (MTT) cell proliferation assay (CellTiter 96 AQ_{eous}; Promega, Madison, WI, USA). In brief, C4-2, DU-145, LNCaP, and PC-3 cancer cells were cultured onto 96-well plates at a density of 5000 cells per well in 100 μL media and allowed to attach overnight. The media in each well was replaced with culture medium containing 2.5–40 μM concentration of CUR and cellulose-CUR. Equivalent amounts of DMSO or cellulose without CUR in PBS were used as control. These plates were incubated at 37 °C for 2 days in an incubator. Then the incubation medium was replaced with 100 μL of fresh medium and 25 μL of MTT reagent and incubated for 3 hrs. The absorbance intensity at 492 nm was recorded using a BioRad microplate reader (BioMate 3 UV-Vis Spectrophotometer, Thermo Electron Corporation, Hudson, NH, USA). The anti-proliferation efficiency of CUR and cellulose-CUR treatments were calculated as a percentage of cell growth with respect to the DMSO and cellulose formulation in PBS controls. From these anti-proliferation values, inhibition concentration (IC_{50}) (concentration of drug required to kill 50% of cells) of CUR and cellulose-CUR formulation is reported. Standard deviations were obtained from 6 replicates.

2.9. Colony Formation Assay

Colony formation assay was employed to assess long-term anti-cancer potential of cellulose-CUR nanoformulation. Briefly, C4-2, DU-145 and PC-3 cancer cells were seeded at a

density of 1000 per well in 6-well plates in 2 mL media and allowed 2 days to start the formation of colonies. Then, media was replaced with different concentrations (2–10 μM) of CUR or cellulose-CUR nanoformulation. After 10 days, these plates were washed three times with PBS, fixed in chilled methanol, stained with hematoxylin (Fisher Scientific, Fair Lawn, NJ, USA), washed with water and air dried. The number of colonies was counted using computer-assisted image analysis with the Multimage™ Cabinet (Alpha Innotech Corporation, San Leandro, CA, USA) and AlphaEase Fc software. The percent colonies were calculated using the number of colonies formed in treatment divided by the number of colonies formed in DMSO or cellulose without CUR in PBS. Standard deviation was obtained from 3 replicates.

2.10. Analysis of Apoptosis

7-Amino actinomycin D (7-AAD) staining was used to detect cellular apoptosis. For this study, C4-2, LNCaP and PC-3 cells were seeded (8×10^5 cells per plate in 10 mL RPMI-1640 medium) into 100 mm Petri dishes and allowed to attach overnight. These cells were treated with 10 mL of 20 μM CUR/cellulose-CUR or equivalent amounts of DMSO/cellulose without CUR in culture medium for 2 days. Following treatments, both adherent and floating cells were collected, washed with PBS, re-suspended in 10 mL culture medium. Cell suspension (1 mL) was incubated with 7 AAD (BD Biosciences, San Diego, CA, USA) at room temperature for 15 min and analyzed by using an Acuri C6 Flow Cytometer (Accuri Cytometers, Inc., Ann Arbor, MI, USA).

3. RESULTS AND DISCUSSION

Several studies indicate that CUR exhibits dose dependant *in vitro* and *in vivo* anti-neoplastic activity against various types of cancers including prostate cancer [24, 40]. The principal CUR delivery issues are its poor solubility, extensive metabolism, low absorption, and dissolution rates [41–43]. A number of CUR analogues and nanoformulation strategies have been developed to overcome these issues which increase their potential impact for cancer treatment [43]. Recent studies of nano- and micro-CUR particles [36, 44–46] have increased CUR levels in the blood and effectively inhibited tumor growth in mouse models. However, it is difficult to recommend any CUR formulation for cancer therapeutics based on drug encapsulation, particle size, stability, solubilization, and bio-availability. Lack of information about the selection of formulation procedure hinders their direct implication for a specific cancer therapy. Therefore, the main aim of the current study was to synthesize, characterize and compare different CUR nanoformulations to identify the best formulation for providing improved cancer cellular uptake and cyto-toxicity effects in clinically relevant prostate cancer cell line models.

Various CUR nanoformulations were prepared according to our previous studies [33, 38, 39]. The encapsulated CUR in the particles varies depending on type of nanoformulation. All these CUR nanoformulations can be suspended in an aqueous solution. TEM demonstrated that nano-CUR formulations have spherical nanoparticles ranging from to ~ 5 – 58 nm while CUR exhibited highly aggregative larger clusters (> 1.2 μm) Fig. (1). The descending order of individual nanoparticle size of formulation is as follows: PLGA NPs-CUR (58.1 nm) > CD-CUR (52.6 nm) > dendrimer-CUR (37.4 nm) > MNP-CUR (8.6 nm) > cellulose-CUR (5.2 nm) Fig. (1). The particles are indicated with black arrows. This study demonstrates that the cellulose-CUR formulation exhibits smallest particle size compared to other CUR nanoformulations.

The presence of CUR in nanoformulations was demonstrated by comparing FTIR spectra of CUR with CUR nanoformulations. FTIR spectra of cellulose, CD, PLGA NPs, MNPs, dendrimer, are shown in Fig. (2A). The FTIR respective peak assignments are given for

cellulose [3440 cm^{-1} (−OH) and 1042 cm^{-1} (C–O–C)], cyclodextrin [3296 cm^{-1} (−OH), 1628 cm^{-1} and 1028 cm^{-1} (C–O and C–O–C of rings of CD)], PLGA NPs [3296 (−OH and −NH) and 1682 cm^{-1} (C-O)], MNP [3296 cm^{-1} (amine groups of MNP surface and −OH of PEO/PPO and CD) 1628 cm^{-1} and 1028 cm^{-1} (C-O and C-O-C of PEO/PPO and CD groups on nanoparticles)] dendrimer [3296 cm^{-1} (−NH), 1637 cm^{-1} (C-O) and 1555 cm^{-1} (C-N)] and presented in Table 2. CUR exhibited prominent peaks at 3510 cm^{-1}, 1515 cm^{-1}, 1273 cm^{-1}, 1116 cm^{-1}, and 955 cm^{-1} Fig. (2B) due to −OH, C-O, C-H, aromatic C-O, and C-O-C stretching vibrations. When CUR was encapsulated in the polymer chain/nanoparticles/dendrimer, prominent peak(s) at 1515 cm^{-1} and 1116 cm^{-1} were evident due to the presence of CUR Fig. (2B) in addition to the parent polymer/nanoparticle/dendrimer spectral peaks. This observation was consistent with FTIR studies of the other polymer based nanoparticles/polymer micelles/polymer encapsulated CUR nanoformulations [34, 35, 45]. The FTIR spectra results indicated that CUR was successfully entrapped into the core structures of the polymeric chains/nanoparticles.

3.1. Physicochemical Characterization

Upon encapsulation of CUR in nanoparticles an increased water solubility and dispersibility was observed. This phenomenon was confirmed by a compatibility study. Since pure CUR is hydrophobic in nature, its aqueous dispersions exhibit a highly disordered and aggregative phenomenon (Fig. (3), black arrows). CUR nanoformulations showed uniform and small aggregate particles (white arrows) or clusters formation (black circles) and aligned structures without aggregates/clusters (white arrows) Fig. (3). MNP and MNP-CUR formulations were not represented because they were difficult to differentiate. This suggests that the microenvironment of CUR in nanoformulations was changed upon encapsulation and this may be due to physical entrapment, inclusion complexation as well as hydrophobic bonding interaction between CUR and polymeric/β-cyclodextrin/dendrimer chains. A similar observation was found with CUR and block copolymer, albumin and polymer nanoparticles [38, 39, 47]. Overall, this study revealed that CUR in nanoformulations exhibited good compatibility.

Further, structural integrity of CUR in nanoformulations was evaluated by X-ray diffraction as well as differential scanning calorimetry. The physicochemical properties of CUR nanoformulations were evaluated using differential scanning calorimetry (DSC) and X-ray diffraction (XRD) studies. These data provide qualitative information and physical state of CUR present in the nanoformulations. The DSC thermogram of CD, cellulose, PLGA NPs, and MNPs has shown their glass transition temperature peak between 50 and 80°C. The DSC thermogram of CUR has shown an intense endothermic peak at 172 °C corresponds to the melting temperature of CUR crystal Fig. (4B). In all CUR nanoformulations, the prominent melting peak belonging to CUR at 172 °C disappeared while their polymer chain/nanoparticle/dendrimer glass transition temperature existed between 50–80°C (Fig. (4B), dotted lines) because CUR molecules are completely entrapped, included and covered by nanoparticle polymeric/β-cyclodextrin/dendrimer chains. The absence of crystalline nature of drug(s) behavior after synthesizing their nanoformulations is due to the drug crystals are completely covered by polymeric/β-cyclodextrin/dendrimer chains [38, 39, 47]. Similar phenomenon was also encountered in various anti-cancer drug nanoformulations [47–49].

X-ray powder diffraction analysis was performed for CUR nanoformulations in comparison with CUR Fig. (5). CUR showed characteristic peaks of diffraction angles 2θ at 8.43°, 11.76°, 14.14°, 16.91°, 17.87°, 20.803°, 23.10°, 24.21°, 25.24°, 26.98°, 27.86° and 28.65°, indicating a highly crystalline state Fig. (5A). These peaks are in good agreement with previous studies reported by different groups as well as the Cambridge Structure Database. After CUR incorporated CUR in nanoparticles, the crystalline peaks of CUR completely disappeared or were hidden due to polymer chain coating of nanoparticles Fig. (5B).

Thereby, amorphous polymer chain layers were more dominant than CUR's crystalline nature. This evidence was also observed in different types of CUR nanoparticles [47–49]. In other words, during the process of CUR nanoformulation, CUR crystalline structure is partly broken down into amorphous phase.

3.2. Evaluation of CUR Nanoformulations for Effective Prostate Cancer Therapy

3.2.1. Cellular Uptake—Desired effects of a drug nanoformulation for superior cancer therapeutics are passive targeting capacity *via* endocytosis and retention/localization at tumor cell(s) or tumor site [50–52]. This experiment was designed to determine the internalization efficacy of various CUR nanoformulations to identify which formulation has a superior cellular uptake in prostate cancer cells. For this study, PC-3 cells were incubated with 10 μM and 20 μM of CUR or CUR nanoformulations for 6 hrs. The ability of internalization was determined utilizing inherent fluorescence property of CUR or CUR in nanoformulations by Flow Cytometry at green fluorescence channel (FL1, 488 excitation, Blue laser, 530 ± 15 nm, FITC/GFP). The order of uptake capacity of CUR and CUR nanoformulations was observed as dendrimer-CUR > cellulose-CUR > CD-CUR > PLGA NPs-CUR > MNP NPs-CUR > CUR at 10 μM and 20 μM concentrations. In detail, 1.25 – 4 (10 μM) and 1.26 – 9.5 (20 μM) fold changes were observed in fluorescence with CUR nanoformulations compared to CUR Fig. (6). Although, the dendrimer-CUR formulation exhibited abundant uptake, it was due to more nanoparticles attached on cancer cells rather internalization. This study reports that the cellulose-CUR nanoformulation shows improved uptake compared to other nanoformulations due to lower particles size. These improved uptake characteristics could exert positive biological effects of CUR and thus the use of cellulose-CUR formulations may be an attractive option for increasing therapeutic efficacy of anti-cancer drugs.

3.2.2. Necrosis/Apoptosis Induction—Apoptosis represents a key factor that is associated with cancer cell death in chemotherapy. The induction of apoptosis can be recognized by various mechanisms including cleaved PARP, activation of casepases and vacuoles or gas vesicles formulation [53–57]. CUR is particularly known to sensitize cells to necrosis. The induction of necrosis/apoptosis was analyzed by TEM analysis of PC-3 cells treated with either 20 μM CUR or CUR nanoformulations for 2 days. An equivalent concentration of nanoformulations without CUR or DMSO was employed as controls. The TEM images of nontreated cells (control formulations without curcumin) showed healthy cellular morphology without any damage or vacuole formation Fig. (7A). CD-CUR, PLGANP-CUR, and cellulose-CUR nanoformulations treatments were able to induce a greater number of vacuole formation throughout the cancer cells compared to CUR treatment Fig. (7). However, the number of vacuole formation in PC-3 cells was: cellulose-CUR ≥ PLGA NP-CUR, > CD-CUR > CUR. Interestingly, even though dendrimer-CUR and MNP-CUR uptake in cancer cells, these formulations showed a distinct change in the overall morphology of PC-cells, not just vacuole formation Fig. (7B). This indicates these formulations acting differently than other CUR nanoformulations. However, a higher number of vacuole formation in the case of the cellulose-CUR nanoformulation it is mainly due to tiny particles which can enter inside the cells *via* endocytosis pathway. Previous findings also illustrate that such higher internalization of CUR nanoformulations always lead to greater anti-cancer potentials [43, 47, 58]. The rest of the CUR nanoformulations demonstrate vacuole formation but are inferior compared to the cellulose-CUR nanoformulation.

From these experiments we conclude that cellulose-CUR nanoformulation may exhibit improved toxicity compared to all other CUR nanoformulations and free CUR due to higher internalization, retention and greater apoptosis in prostate cancer cells. We believe that the

cellulose-CUR nanoformulation will be a better therapeutic strategy to treat prostate cancers and thus all further studies were conducted using cellulose-CUR nanoformulations. To confirm the applicability of the cellulose-CUR nanoformulation in cancer treatment, these nanoparticles were investigated for *in vitro* anti-cancer properties such as a standard cell proliferation assay (MTT assay), clonogenic (colony formation) assay, and apoptosis assay (7-AAD staining) in human prostate cancer cells.

3.3. Anti-Cancer Potential of Cellulose-CUR Formulation

Various CUR encapsulated nanoformulations revealed variations in their anti-cancer activities [43], dependent upon their direct interaction of CUR nanoformulations with cancer cells or CUR release characteristic from nanoformulations. On the other hand, many CUR nanoformulations exhibited improved or comparable activities to DMSO-dissolved CUR. Therefore, we evaluated *in vitro* anti-cancer efficacy of the cellulose-CUR nanoformulation and compared it with free CUR.

3.3.1. Improved Anti-Cancer Characteristics of Cellulose-CUR Formulation— To determine anti-cancer potential of free CUR and cellulose-CUR nanoformulation, a standard cell proliferation assay (MTT assay) was performed on a panel of four prostate cancer cell lines [C4-2, DU-145, LNCaP and PC-3]. These cells were incubated with 2.5–40 μM of free CUR or cellulose-CUR nanoformulations for 2 days and then examined for cell viability. Cells treated with equivalent amounts of DMSO or cellulose without CUR were used as controls for CUR and cellulose-CUR formulation, respectively. There was no effect on cancer cell proliferation with controls treatment while both CUR and the cellulose-CUR formulation exhibited dose dependant anti-cancer effects in prostate cancer cells. At all the concentrations of nanocurcumin exhibited competitive equivalent anti-cancer potential compared to curcumin Fig. (8A) but the effect is not synergistic in nature. The inhibitory concentration (IC_{50}) was: 11.5 ± 4.2 μM, 18.2 ± 2.6 μM, 37.4 ± 3.2 μM, 26.2 ± 3.4 μM for CUR and 7.8 ± 1.78 μM, 17.5 ± 2.65 μM, 30.1 ± 1.9 μM, 19.8 ± 2.8 μM for cellulose-CUR formulation treatments on C4-2, DU-145, LNCaP and PC-3, respectively Fig. (8B). This experiment suggests greater anti-proliferative effects of cellulose-CUR formulation compared to free CUR.

Colony formation assay was employed to evaluate the long term anti-cancer potential of cellulose-CUR nanoformulation. In this study, C4-2, DU145 and PC3 cancer cell lines were treated with equivalent doses of 4 and 8 μM CUR or cellulose-CUR nanoformulation. Equivalent quantities of DMSO or cellulose were used as control for CUR and cellulose-CUR nanoformulation, respectively. The colony formation data exhibited improved therapeutic efficacy of cellulose-CUR nanoformulation in all three cell lines compared to free CUR Fig. (9). The enhanced anti-cancer therapeutic efficacy of cellulose-CUR nanoformulation compared to free CUR is due to slow release of CUR from internalized cellulose-CUR nanoparticles in prostate cancer cells.

3.3.2. 7-Amino Actinomycin D (7-AAD) Staining—Unlike conventional chemotherapeutic drugs, CUR induces apoptosis in both androgen-dependent and androgen-independent prostate cancer cells. This process occurs through intrinsic (mitochondrial) *via* stress or DNA damage, extrinsic (receptor-mediated) pathways, and stress of the endoplasmic reticulum. Several investigations including our reports revealed that CUR and CUR nanoformulations are capable to down-regulate pro-survival proteins such as Bcl-2 and Bcl-xL and enhance cleavage of PARP protein (apoptosis marker) which eventually leads to cellular apoptosis in cancer cells [43, 47, 54, 56, 59].

This apoptosis feature of CUR occurs due to increased permeability or disruption of cell membranes that allow it to interact at molecular levels, rendering cancer cell death. In our current study, we investigated a sensitive detection of apoptosis by Flow Cytometry. In this procedure, apoptotic and or necrotic cells which have lost membrane integrity or porous membranes, take up the 7-AAD and intercalate into double-stranded nucleic acids (DNA). 7-AAD can easily penetrate through cell membranes of dying or dead cells. The quantification of 7-AAD stain in cancer cells treated with 20 μM cellulose-CUR nanoformulation showed 2 – 4 fold higher than those treated with free CUR Fig. (10), indicating cellulose-CUR formulation is a promising therapeutic agent for prostate cancer. Our prior studies also demonstrated that CUR nanoformulations have potent anti-cancer characteristics in cancer cells [29, 33].

In summary, our data reports that cellulose-CUR nanoformulation exhibited superior anti-cancer properties. The Food and Drug Administration (FDA) considers cellulose polymers to be safe (GRAS) when used in number of food, ophthalmic, cosmetic, drug additive, and adhesive products. In addition, cellulose used in this study is highly employed by the pharmaceutical industry to make pills and gel capsules. The novel cellulose-CUR nanoparticle formulation developed in this study holds the potential to advance to pre-clinical animal studies and to clinical studies. Further, the available functional hydroxyl groups of cellulose, their CUR nanoformulations, can be utilized for immunoconjugation for efficient tumor targeted delivery.

4. CONCLUSION

Developing a suitable CUR nanoformulation for efficient prostate cancer therapy is a challenge. For this, we scrutinized various nanoformulations of CUR for superior anti-cancer effects in prostate cancer treatment. Among CUR, PLGA, β-cyclodextrin, cellulose, dendrimer and magnetic nanoparticle based nano-CUR formulations, the cellulose-CUR nanoformulation exhibited significantly higher intracellular uptake as well anti-cancer efficacy. Our results suggest the cellulose-CUR formulation possesses characteristics which will improve the therapeutic treatment of prostate cancer; however, further pre clinical and clinical studies are warranted in future.

Acknowledgments

We thank Cathy Christopherson (Sanford Research/USD, Sioux Falls) for editorial assistance, Robert Japs (Sanford Health, Flow Cytometry Core, Sanford Research/USD), Sara Basiaga (Department of Chemistry, UN-Lincoln) and Shah R Valloppilly (Nebraska Center for Materials and Nanoscience, Department of Physics and Astronomy, UN-Lincoln), for their help in characterization of our samples. This work was supported by grants from Sanford Research/USD, Department of Defense (DOD) (PC073887), Governor's Cancer 2010, and NIH RO1 (CA142736) awarded to SCC and Department of Defense (DOD) (PC073643) and Governor's Cancer 2010 grants awarded to MJ.

References

1. Centers for disease control and prevention, National program of cancer registries (NPCR). [Accessed April 25, 2011] Top ten cancers in United States. 2007. http://apps.nccd.cdc.gov/uscs/toptencancers.aspx
2. Jemal A, Siegel R, Ward E, Hao Y, Xu J, Thun MJ. Cancer statistics, 2009. CA Cancer J Clin. 2009; 59:225–249. [PubMed: 19474385]
3. Teiten MH, Gaascht F, Eifes S, Dicato M, Diederich M. Chemopreventive potential of curcumin in prostate cancer. Genes Nutr. 2010; 5:61–74. [PubMed: 19806380]
4. Al-Mamgani A, Lebesque JV, Heemsbergen WD, Tans L, Kirkels WJ, Levendag PC, Incrocci L. Controversies in the treatment of high-risk prostate cancer--what is the optimal combination of

hormonal therapy and radiotherapy: a review of literature. Prostate. 2010; 70:701–709. [PubMed: 20017166]

5. Dal Pra A, Cury FL, Souhami L. Combining radiation therapy and androgen deprivation for localized prostate cancer-a critical review. Curr Oncol. 2010; 17:28–38. [PubMed: 20975876]
6. Kohli M, Tindall DJ. New developments in the medical management of prostate cancer. Mayo Clin Proc. 2010; 85:77–86. [PubMed: 20042563]
7. Moore CM, Pendse D, Emberton M. Photodynamic therapy for prostate cancer--a review of current status and future promise. Nat Clin Pract Urol. 2009; 6:18–30. [PubMed: 19132003]
8. Peschel RE, Robnett TJ, Hesse D, King CR, Ennis RD, Schiff PB, Wilson LD. PSA based review of adjuvant and salvage radiation therapy vs. observation in postoperative prostate cancer patients. Int J Cancer. 2000; 90:29–36. [PubMed: 10725855]
9. Quon H, Loblaw DA. Androgen deprivation therapy for prostate cancer-review of indications in 2010. Curr Oncol. 2010; 17:S38–44. [PubMed: 20882131]
10. Roscigno M, Sangalli M, Mazzoccoli B, Scattoni V, Da Pozzo L, Rigatti P. Medical therapy of prostate cancer. A review. Minerva Urol Nefrol. 2005; 57:71–84. [PubMed: 15951731]
11. Beer TM, Bubalo JS. Complications of chemotherapy for prostate cancer. Semin Urol Oncol. 2001; 19:222–230. [PubMed: 11561990]
12. Heidenreich A, von Knobloch R, Hofmann R. Current status of cytotoxic chemotherapy in hormone refractory prostate cancer. Eur Urol. 2001; 39:121–130. [PubMed: 11223670]
13. Pomerantz M, Kantoff P. Advances in the treatment of prostate cancer. Annu Rev Med. 2007; 58:205–220. [PubMed: 16987081]
14. Rauchenwald M, De Santis M, Fink E, Holtl W, Kramer G, Marei IC, Neumann HJ, Reissigl A, Schmeller N, Stackl W, Hobisch A, Krainer M. Chemotherapy for prostate cancer. Wien Klin Wochenschr. 2008; 120:440–449. [PubMed: 18726672]
15. Amato RJ, Teh BS, Henary H, Khan M, Saxena S. A retrospective review of combination chemohormonal therapy as initial treatment for locally advanced or metastatic adenocarcinoma of the prostate. Urol Oncol. 2009; 27:165–169. [PubMed: 18367115]
16. Letsch M, Schally AV, Szepeshazi K, Halmos G, Nagy A. Effective treatment of experimental androgen sensitive and androgen independent intraosseous prostate cancer with targeted cyto-toxic somatostatin analogue AN-238. J Urol. 2004; 171:911–915. [PubMed: 14713852]
17. Small EJ. Advances in prostate cancer. Curr Opin Oncol. 1999; 11:226–235. [PubMed: 10328599]
18. Fitzpatrick JM. The application of nanotechnology for the treatment of metastatic prostate cancer. BJU Int. 2009; 104:i. [PubMed: 19706031]
19. Gommersall L, Shergill IS, Ahmed HU, Arya M, Grange P, Gill IS. Nanotechnology in the management of prostate cancer. BJU Int. 2008; 102:1493–1495. [PubMed: 18990144]
20. Michael A, Syrigos K, Pandha H. Prostate cancer chemotherapy in the era of targeted therapy. Prostate Cancer Prostatic Dis. 2009; 12:13–16. [PubMed: 18521103]
21. Kuttan R, Sudheeran PC, Josph CD. Turmeric and curcumin as topical agents in cancer therapy. Tumori. 1987; 73:29–31. [PubMed: 2435036]
22. Shishodia S, Chaturvedi MM, Aggarwal BB. Role of curcumin in cancer therapy. Curr Probl Cancer. 2007; 31:243–305. [PubMed: 17645940]
23. Thangapazham RL, Puri A, Tele S, Blumenthal R, Maheshwari RK. Evaluation of a nanotechnology-based carrier for delivery of curcumin in prostate cancer cells. Int J Oncol. 2008; 32:1119–1123. [PubMed: 18425340]
24. Anand P, Sundaram C, Jhurani S, Kunnumakkara AB, Aggarwal BB. Curcumin and cancer: an “old-age” disease with an “age-old” solution. Cancer Lett. 2008; 267:133–164. [PubMed: 18462866]
25. Hatcher H, Planalp R, Cho J, Torti FM, Torti SV. Curcumin: from ancient medicine to current clinical trials. Cell Mol Life Sci. 2008; 65:1631–1652. [PubMed: 18324353]
26. Kunnumakkara AB, Anand P, Aggarwal BB. Curcumin inhibits proliferation, invasion, angiogenesis and metastasis of different cancers through interaction with multiple cell signaling proteins. Cancer Lett. 2008; 269:199–225. [PubMed: 18479807]

27. Landis-Piwowar KR, Milacic V, Chen D, Yang H, Zhao Y, Chan TH, Yan B, Dou QP. The proteasome as a potential target for novel anticancer drugs and chemosensitizers. Drug Resist Update. 2006; 9:263–273.
28. Page P, Yang LX. Novel chemoradiosensitizers for cancer therapy. Anticancer Res. 2010; 30:3675–3682. [PubMed: 20944153]
29. Yallapu MM, Maher DM, Sundram V, Bell MC, Jaggi M, Chauhan SC. Curcumin induces chemo/radio-sensitization in ovarian cancer cells and curcumin nanoparticles inhibit ovarian cancer cell growth. J Ovarian Res. 2010; 3:11. [PubMed: 20429876]
30. Um Y, Cho S, Woo HB, Kim YK, Kim H, Ham J, Kim SN, Ahn CM, Lee S. Synthesis of curcumin mimics with multidrug resistance reversal activities. Bioorg Med Chem. 2008; 16:3608–3615. [PubMed: 18295490]
31. Strimpakos AS, Sharma RA. Curcumin: preventive and therapeutic properties in laboratory studies and clinical trials. Antioxid Redox Signal. 2008; 10:511–545. [PubMed: 18370854]
32. Gosangari, SL.; Watkin, KL. Effect of preparation techniques on the properties of curcumin liposomes: Characterization of size, release and cytotoxicity on a squamous oral carcinoma cell line. Pharm Dev Technol. 2011. [http://informahealthcare.com/doi/abs/10.3109/10837450.2010.522583]
33. Yallapu MM, Gupta BK, Jaggi M, Chauhan SC. Fabrication of curcumin encapsulated PLGA nanoparticles for improved therapeutic effects in metastatic cancer cells. J Colloid Interface Sci. 2010; 351:19–29. [PubMed: 20627257]
34. Konwarh R, Saikia JP, Karak N, Konwar BK. 'Poly(ethylene glycol)-magnetic nanoparticles-curcumin' trio: directed morphogenesis and synergistic free-radical scavenging. Colloids Surf B: Biointerfaces. 2010; 81:578–586. [PubMed: 20729041]
35. Bisht S, Feldmann G, Soni S, Ravi R, Karikar C, Maitra A, Maitra A. Polymeric nanoparticle-encapsulated curcumin ("nanocurcumin"): a novel strategy for human cancer therapy. J Nanobiotechnology. 2007; 5:3. [PubMed: 17439648]
36. Bisht S, Mizuma M, Feldmann G, Ottenhof NA, Hong SM, Pramanik D, Chenna V, Karikari C, Sharma R, Goggins MG, Rudek MA, Ravi R, Maitra A, Maitra A. Systemic administration of polymeric nanoparticle-encapsulated curcumin (NanoCurc) blocks tumor growth and metastases in preclinical models of pancreatic cancer. Mol Cancer Ther. 2010; 9:2255–2264. [PubMed: 20647339]
37. Yallapu MM, Jaggi M, Chauhan SC. Scope of nanotechnology in ovarian cancer therapeutics. J Ovarian Res. 2010; 3:19. [PubMed: 20691083]
38. Yallapu MM, Othman SF, Curtis ET, Gupta BK, Jaggi M, Chauhan SC. Multi-functional magnetic nanoparticles for magnetic resonance imaging and cancer therapy. Biomaterials. 2011; 32:1890–1905. [PubMed: 21167595]
39. Yallapu MM, Jaggi M, Chauhan SC. beta-Cyclodextrin-curcumin self-assembly enhances curcumin delivery in prostate cancer cells. Colloids Surf B: Biointerfaces. 2010; 79:113–125. [PubMed: 20456930]
40. Aggarwal BB, Sung B. Pharmacological basis for the role of curcumin in chronic diseases: an age-old spice with modern targets. Trends Pharmacol Sci. 2009; 30:85–94. [PubMed: 19110321]
41. Ireson CR, Jones DJ, Orr S, Coughtrie MW, Boocock DJ, Williams ML, Farmer PB, Steward WP, Gescher AJ. Metabolism of the cancer chemopreventive agent curcumin in human and rat intestine. Cancer Epidemiol Biomarkers Prev. 2002; 11:105–111. [PubMed: 11815407]
42. Ireson C, Orr S, Jones DJ, Verschoyle R, Lim CK, Luo JL, Howells L, Plummer S, Jukes R, Williams M, Steward WP, Gescher A. Characterization of metabolites of the chemopreventive agent curcumin in human and rat hepatocytes and in the rat *in vivo*, and evaluation of their ability to inhibit phorbol ester-induced prostaglandin E2 production. Cancer Res. 2001; 61:1058–1064. [PubMed: 11221833]
43. Anand P, Kunnumakkara AB, Newman RA, Aggarwal BB. Bioavailability of curcumin: problems and promises. Mol Pharm. 2007; 4:807–818. [PubMed: 17999464]
44. Shahani K, Swaminathan SK, Freeman D, Blum A, Ma L, Panyam J. Injectable sustained release microparticles of curcumin: a new concept for cancer chemoprevention. Cancer Res. 2010; 70:4443–4452. [PubMed: 20460537]

45. Shahani K, Panyam J. Highly loaded, sustained-release microparticles of curcumin for chemoprevention. J Pharm Sci. 2011; 100:2599–2609. [PubMed: 21547911]
46. Lim KJ, Bisht S, Bar EE, Maitra A, Eberhart CG. A polymeric nanoparticle formulation of curcumin inhibits growth, clonogenicity and stem-like fraction in malignant brain tumors. Cancer Biol Ther. 2011; 11:464– 473. [PubMed: 21193839]
47. Mulik RS, Monkkonen J, Juvonen RO, Mahadik KR, Paradkar AR. Transferrin mediated solid lipid nanoparticles containing curcumin: Enhanced *in vitro* anticancer activity by induction of apoptosis. Int J Pharm. 2010; 398:190–203. [PubMed: 20655375]
48. Mohanty C, Sahoo SK. The *in vitro* stability and *in vivo* pharmacokinetics of curcumin prepared as an aqueous nanoparticulate formulation. Biomaterials. 2010; 31:6597–6611. [PubMed: 20553984]
49. Merisko-Liversidge EM, Liversidge GG. Drug nanoparticles: formulating poorly water-soluble compounds. Toxicol Pathol. 2008; 36:43–48. [PubMed: 18337220]
50. Pridgen EM, Langer R, Farokhzad OC. Biodegradable, polymeric nanoparticle delivery systems for cancer therapy. Nanomedicine. 2007; 2:669–680. [PubMed: 17976029]
51. Krishnan S, Diagaradjane P, Cho SH. Nanoparticle-mediated thermal therapy: evolving strategies for prostate cancer therapy. Int J Hyperthermia. 2010; 26:775–789. [PubMed: 20858069]
52. Brannon-Peppas L, Blanchette JO. Nanoparticle and targeted systems for cancer therapy. Adv Drug Deliv Rev. 2004; 56:1649–1659. [PubMed: 15350294]
53. Araki T, Hayashi M, Saruta T. Anion-exchange blocker enhances cytoplasmic vacuole formation and cell death in serum-deprived mouse kidney epithelial cells in mice. Cell Biol Int. 2006; 30:93–100. [PubMed: 16376114]
54. Brauns SC, Dealtry G, Milne P, Naude R, Van de Venter M. Caspase-3 activation and induction of PARP cleavage by cyclic dipeptide cyclo(Phe-Pro) in HT-29 cells. Anticancer Res. 2005; 25:4197–4202. [PubMed: 16309216]
55. Yang SE, Hsieh MT, Tsai TH, Hsu SL. Down-modulation of Bcl-XL, release of cytochrome c and sequential activation of caspases during honokiol-induced apoptosis in human squamous lung cancer CH27 cells. Biochem Pharmacol. 2002; 63:1641–1651. [PubMed: 12007567]
56. Choi YH, Kong KR, Kim YA, Jung KO, Kil JH, Rhee SH, Park KY. Induction of Bax and activation of caspases during beta-sitosterol-mediated apoptosis in human colon cancer cells. Int J Oncol. 2003; 23:1657–1662. [PubMed: 14612938]
57. Mahmoudi M, Simchi A, Imani M, Shokrgozar MA, Milani AS, Hafeli UO, Stroeve P. A new approach for the *in vitro* identification of the cytotoxicity of superparamagnetic iron oxide nanoparticles. Colloids Surf B: Biointerfaces. 2010; 75:300–309. [PubMed: 19781921]
58. Anitha A, Maya S, Deepa N, Chennazhi KP, Nair SV, Tamura H, Jayakumar R. Efficient water soluble O-carboxymethyl chitosan nanocarrier for the delivery of curcumin to cancer cells. Carbohyd Polym. 2011; 83:452–461.
59. Yadav VR, Prasad S, Kannappan R, Ravindran J, Chaturvedi MM, Vaahtera L, Parkkinen J, Aggarwal BB. Cyclodextrin-complexed curcumin exhibits anti-inflammatory and antiproliferative activities superior to those of curcumin through higher cellular uptake. Biochem Pharmacol. 2010; 80:1021–1032. [PubMed: 20599780]

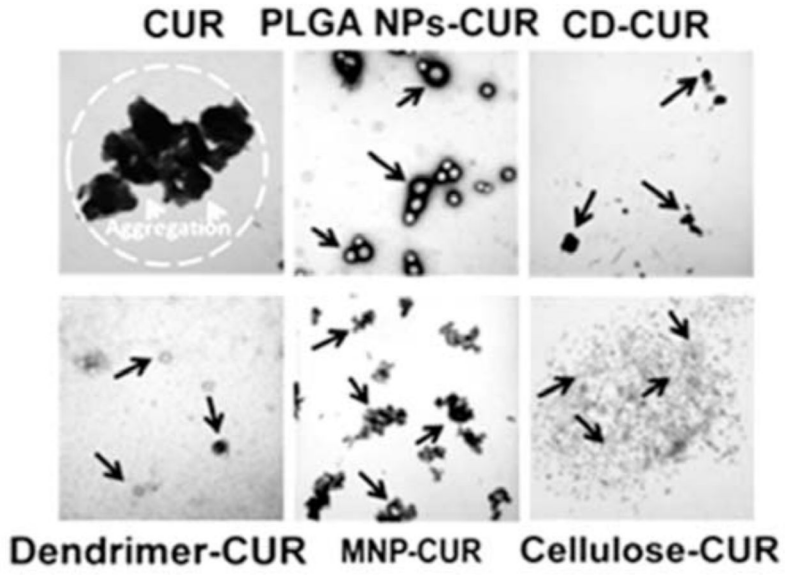

Fig. 1.

TEM images of CUR, CD-CUR, cellulose-CUR, PLGA NPs-CUR, MNP-CUR and dendrimer-CUR nanoformulations. Particles were dispersed in water and 2–3 drops were place on 200 mesh formvar-coated copper grid and imaged at 80 kV. Bar line indicates 200 nm for all images.

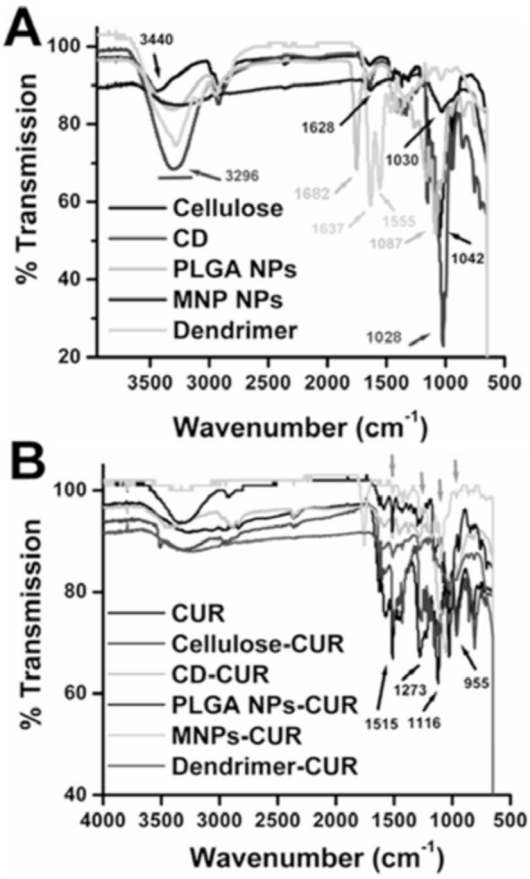

Fig. 2.
FTIR spectra of various polymer/nanoparticles, CUR and CUR nanoformulations. Spectra of solid powders were recorded on ATR-FTIR plate.

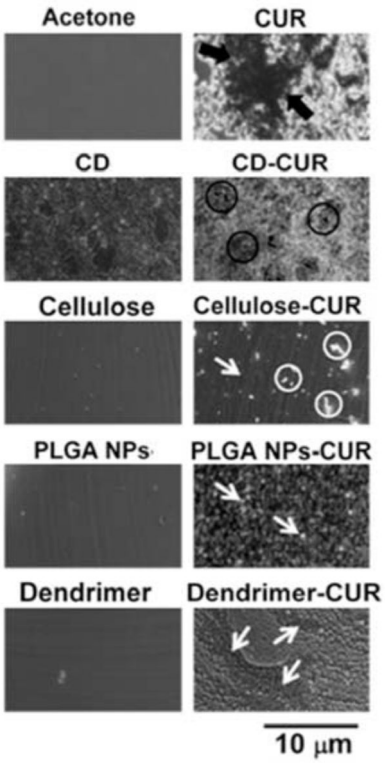

Fig. 3.
Optical microscopic images of various solvent, polymers/nanoparticles, CUR and CUR nanoformulation films obtained from aqueous solutions. Bar line indicates 10 microns for all images.

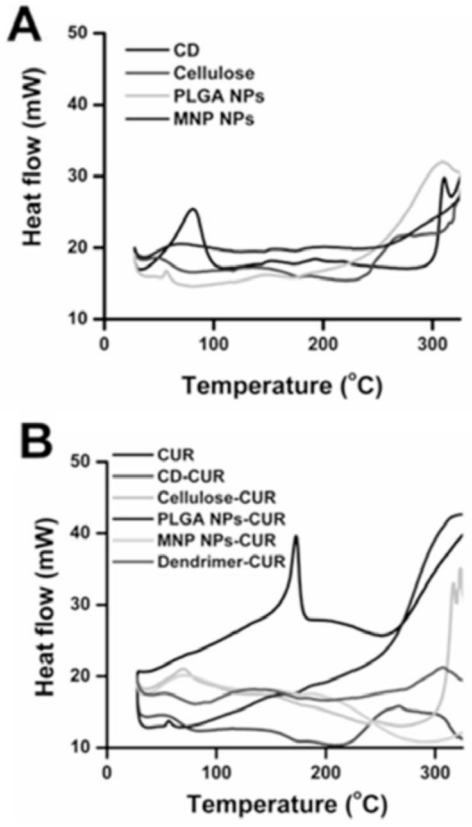

Fig. 4.
DSC thermograms of polymer/nanoparticles, CUR and CUR nanoformulations. Heating rate is 10°C per min.

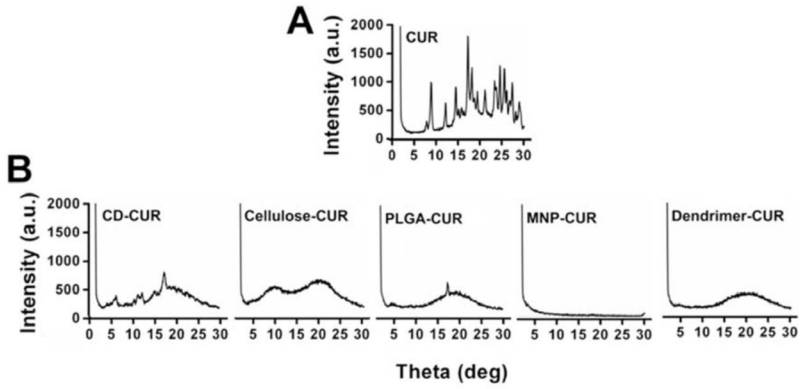

Fig. 5.

X-ray diffraction patterns of CUR and CD-CUR, cellulose-CUR, PLGA-CUR, MNP-CUR and dendrimer CUR nanoformulations.

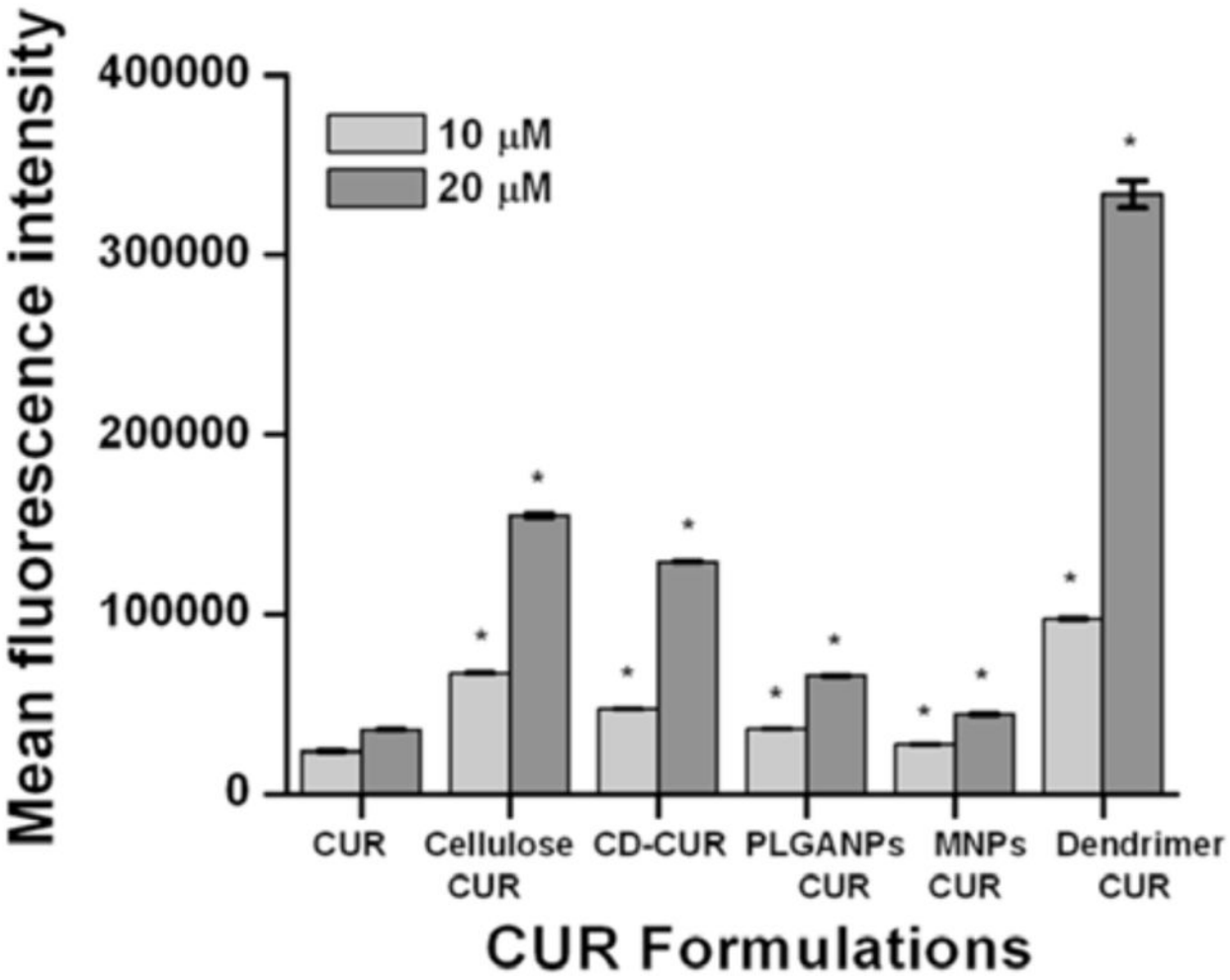

Fig. 6.

Cellular uptake of CUR and CUR nanoformulations in PC-3 cancer cells. Cells (5×10^5) were treated with 10 μM or 20 μM of CUR or equivalent CUR nanoformulations for 6 hrs. Mean fluorescence of cells was measured by Accuri Flow Cytometer. Data represents average of 3 repeats. *$p < 0.05$ represents significant difference from the CUR uptake. **Note:** Although dendrimer exhibited higher fold change in fluorescence it is attributed to the attached CUR formulation on the cancer cells, not internalization.

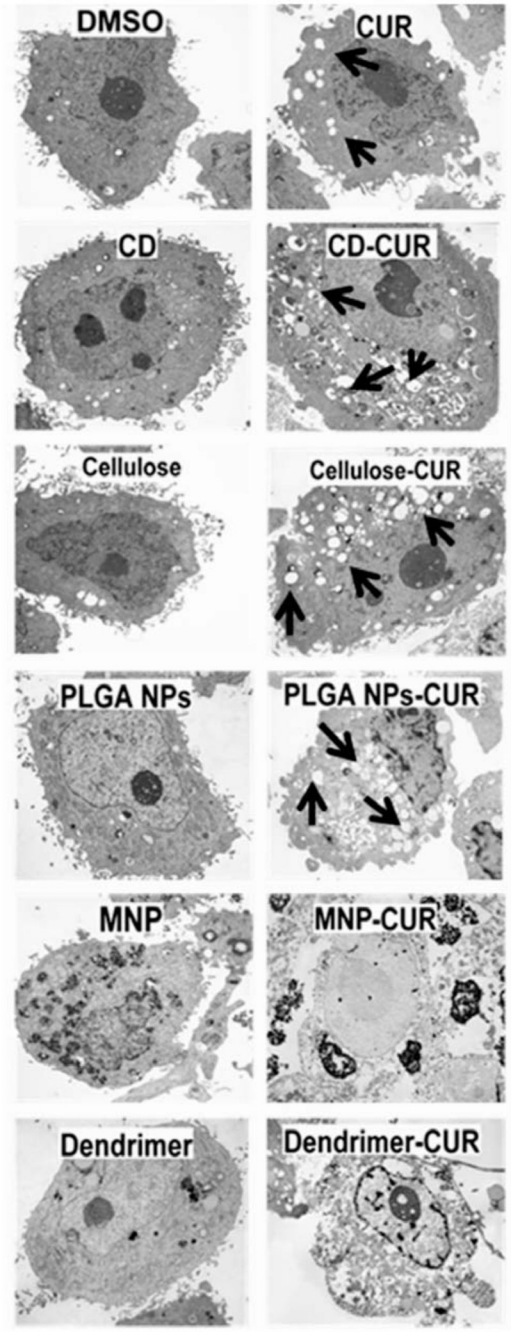

Fig. 7.

Transmission electron micrographs revealing the treatment effect on ultra structural cellular changes in PC-3 cancer cells in DMSO control, polymer/nanoparticles, CUR and CUR nanoformulations. Black arrows indicate vacuoles. A distinct morphology with different contrast was observed with MNP-CUR and dendrimer-CUR formulation treatment.

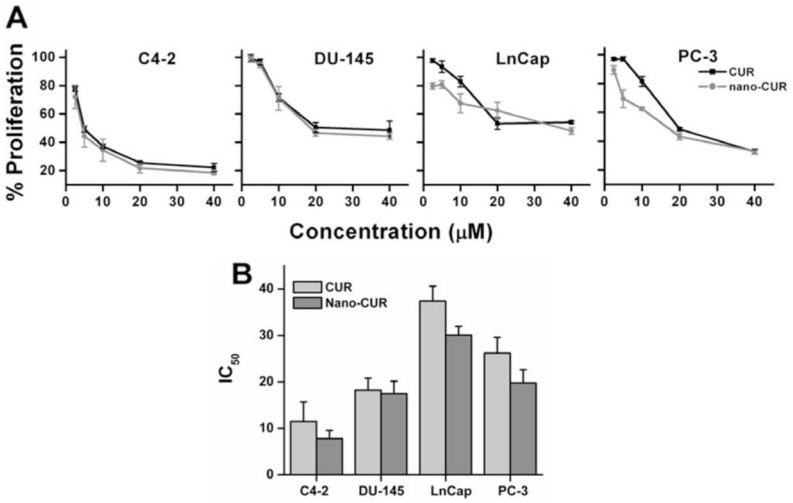

Fig. 8.

Anti-cancer potential of nanocurcumin in prostate cancer cells. (**A**) Anti-proliferative effect of CUR and cellulose-CUR treatment in C4-2, DU-145, LNCaP, and PC-3 cancer cells (**A**). Cells were treated with CUR or cellulose-CUR and on day 2 cell viability was measured by MTT assay using UV-vis spectrophotometer at 492 nm. Data is mean ± SEM (n = 6). DMSO and cellulose were used as controls. (**B**) IC_{50} values obtained from the proliferation experiments.

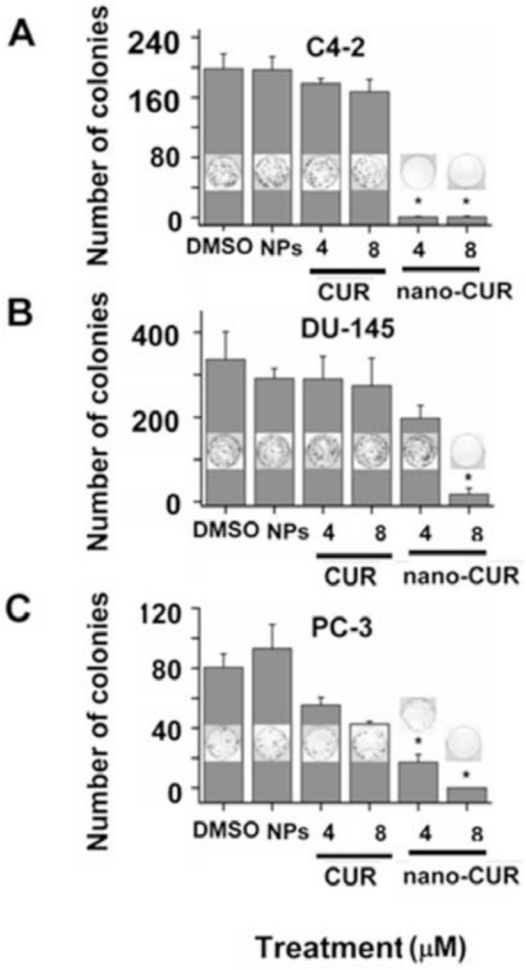

Fig. 9.

Colony formation assays of prostate cancer cells treated with CUR or cellulose-CUR. Data represent mean of 3 repeats for each treatment, mean ± SEM (n = 3). DMSO and cellulose control did not show any effect on colony formation. Note: LNCaP cells have difficulty forming colonies and therefore are not used in this assay.

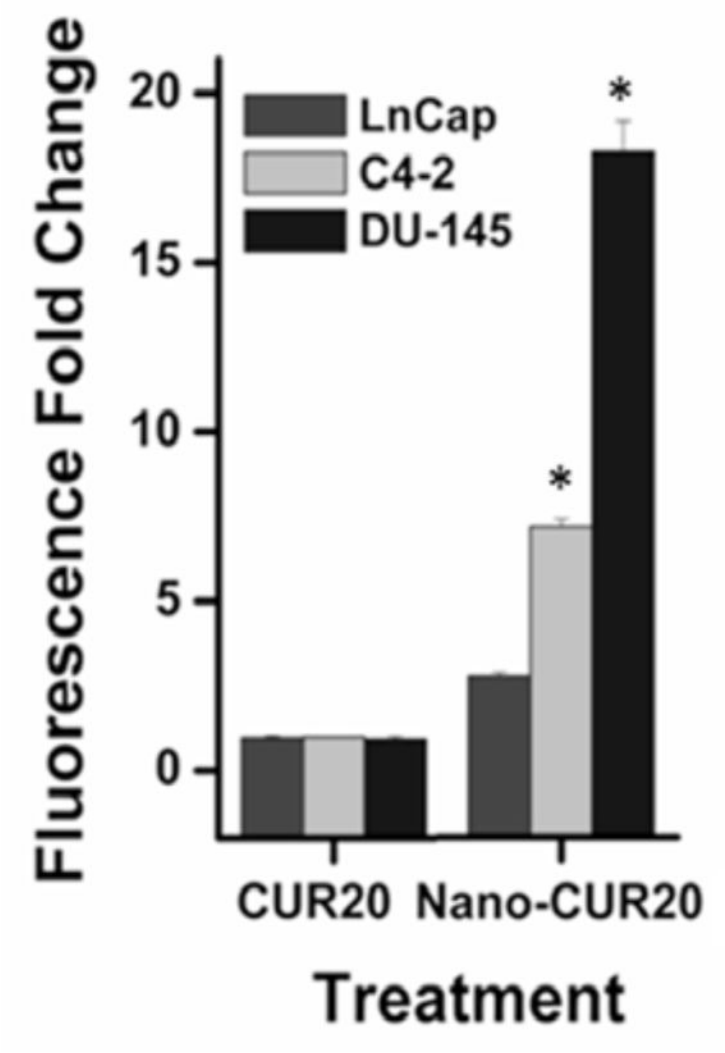

Fig. 10.
Analysis of cellular apoptosis by CUR and cellulose-CUR treatment (7AAD positive cells). Data represent mean of 3 repeats for each treatment (Mean ± SE; *$p < 0.05$, compared to the equivalent dose of curcumin).